European Journal of Histochemistry 2025; volume 69:4244

Immunohistochemical analysis of YB-1 expression in the developing mouse eye

Alexander Florian Nass,[1] Hella Wolf,[2] Saadettin Sel,[3] Thomas Kalinski,[1] Norbert Nass[1,2]

[1]Brandenburg Medical School Theodor Fontane (MHB), University Hospital Brandenburg/Havel, Institute of Pathology, Brandenburg/Havel
[2]Institute of Pathology, Otto von Guericke University, Magdeburg
[3]Department of Ophthalmology, University of Heidelberg, Germany

ABSTRACT

Cold shock domain (CSD) proteins, such as YB-1, play a crucial role in the regulation of transcription, mRNA stability, and translation. Consequently, YB-1 is implicated in processes such as cell differentiation, oncogenesis and oxidative stress response. The development of the eye is a complex process that involves the differentiation of numerous highly specialized cell types. We hypothesized that YB-1 is involved in both eye development and stress defense mechanisms. As an initial step, we investigated the expression of YB-1 during the embryology of the mouse eye. YB-1 mRNA could be detected by RT-PCR and sequencing the PCR product in retinal tissue of adult mice. To elucidate the expression pattern of YB-1 protein during mouse eye development, we analyzed its expression in the developing mouse eye at embryonic day 13 (E13), E15, E18 and postnatal day 14 (P14) using immunohistochemistry. Expression of the YB-1 protein was detected in all retinal cells, as well as in the corneal and lens epithelial cells, throughout all stages of eye development examined. These findings suggest that YB-1 could have a significant role in the eye, potentially related to development and differentiation.

Key words: eye; development; YB-1; immunohistochemistry; cornea; retina.

Correspondence: Norbert Nass, Brandenburg Medical School Theodor Fontane (MHB), University Hospital Brandenburg/Havel, Institute of Pathology, Hochstr. 29, D-14770 Brandenburg/Havel, Germany.
E-mail: Norbert.nass@mhb-fontane.de

Contributions: AFN, HW, investigation; NN: conceptualisation, methodology, writing original draft; SS, methodology, writing review and editing; TK, conceptualisation, writing original draft, supervision.

Conflict of interest: the authors declare no competing interests and all authors confirm accuracy.

Ethics approval: the animal experiments have been approved by the animal welfare committee of the Martin-Luther University Halle-Wittenberg (Reference K1/T1-11(M4))

Availability of data and materials: the datasets used and/or analyzed during the current study are available upon reasonable request from the corresponding author.

Funding: research of NN and TK are supported by the Ministry of Science, Research and Cultural Affairs of the State of Brandenburg.

Introduction

The mammalian eye is a highly specialized organ, comprising several highly dedicated cells. During the embryogenesis, it originates from cells of the mesenchyme, ectoderm, and neural crest.[1] Specifically, the retina, iris, ciliary body, and nerves are derived from neural epithelial cells,[2] while the cornea and lens develop from the surface ectoderm.[3] The vitreous and sclera are formed from mesenchymal cells.[4,5] This entire developmental process is primarily driven by well-organized sequential events.[6]

The vertebrate neuroretina is a multi-layered tissue responsible for light perception and initial signal processing.[2] Six types of retinal cells contribute to its structure: photoreceptors (classified as rod and cone cells), amacrine cells, horizontal cells, bipolar cells, and ganglion cells, along with three types of glial cells, namely astrocytes, Müller cells, and resident microglia. These cells form a highly organized structure with three nuclear layers separated by two plexiform layers. The inner nuclear layer (INL) contains the nuclei of amacrine, Müller glia, horizontal, and bipolar cells.[7] The outer nuclear layer (ONL) comprises the nuclei of photoreceptor cells. The ganglion cell layer (GCL) consists of displaced amacrine and ganglion cells. These three layers are separated by the inner (IPL) and outer plexiform (OPL) layers, which contain axons and dendrites connecting the neuronal cells of the nuclear layers. The entire structure develops from a pool of pluripotent stem cells in a chronological order.[8,9] Initially, retinal ganglion cells are formed, followed by overlapping stages where horizontal cells, cone photoreceptors, amacrine cells, rod photoreceptors, bipolar cells, and Müller glia cells differentiate.[10] The cornea originates from cells of the surface ectoderm.[11] This transparent tissue consists of the corneal epithelium (CEpi), endothelium (CEndo), and stroma (CS). The CS is further embedded between two acellular structures called Bowman's and Descemet's membranes.[12] The lens is also a derivative of the surface epithelium. During mouse development, around embryonic day 10 (E10), the lens ectoderm invaginates and forming lens pit and vesicle.[1] The fibroblasts of the CS and the CEndo cells both derive from mesenchymal cells originating from the neural crest.[13] The cornea, lens, and vitreous are transparent structures that allow light to reach the retinal tissue. Consequently, these tissues are constantly exposed to stress, particularly from reactive oxygen species generated by absorbed photons.[14] This exposure leads to oxidative modifications and glycation. As a defense mechanism, the vitreous and lens contain significant amounts of ascorbic acid and other antioxidants.[15]

The Y-box binding protein 1 (YB-1), also known as the Y-box transcription factor, is encoded in mice by the *Ybx1* gene and belongs to the highly conserved cold shock domain (CSD) protein family.[16] This domain is essential to DNA and RNA binding. The protein plays a role in regulating both transcription and translation, it impacts DNA repair, drug resistance, and stress responses. Predominantly localized in the cytosol, YB-1 can translocate to the nucleus, often contingent upon modifications such as phosphorylation and acetylation.[17,18] Additionally, YB-1 is found extracellularly and contributes to exosome formation.[19] While the expression of *Ybx1* mRNA in the mouse eye has been previously reported,[20] to our best knowledge, a comprehensive expression analysis in the developing eye has not been published.

Our objective was therefore to investigate the expression pattern of YB-1 in the developing mouse eye. Therefore, we analysed its expression in the mouse eye at embryonic stages E13, E15, and E18, as well as in postnatal day 14 (P14).

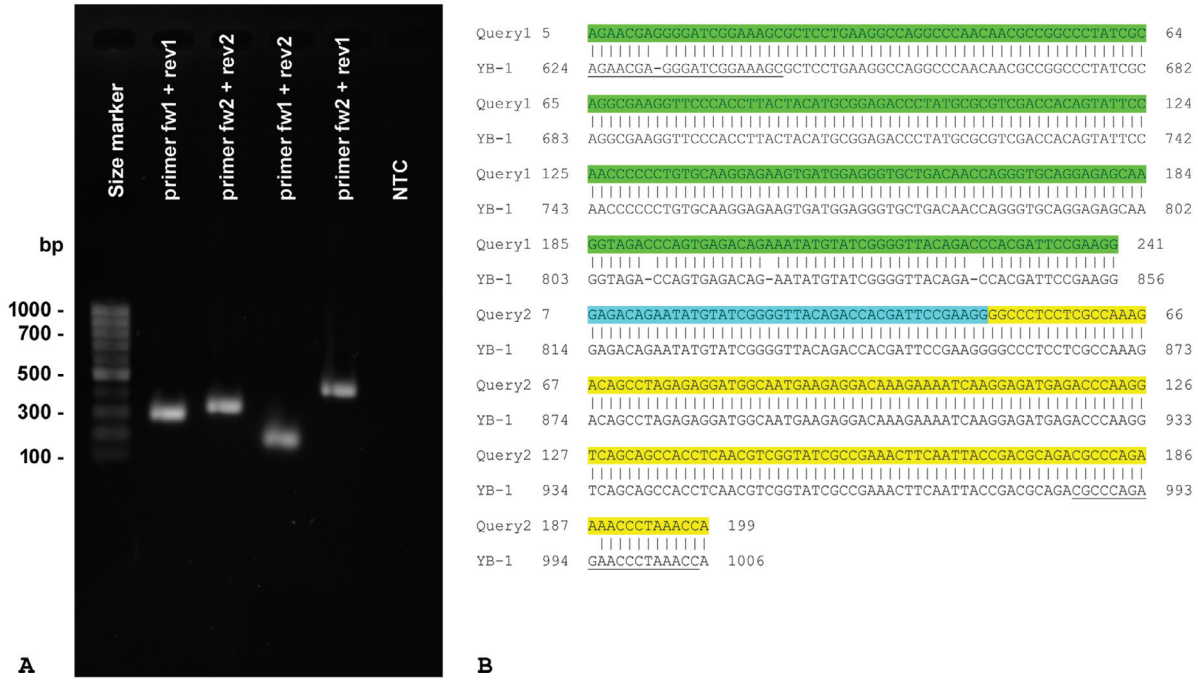

Figure 1. YB-1 mRNA is expressed in adult neuroretinal cells. **A**) RT-PCR analysis showing *YB-1* gene products from adult retina; the DNA marker (M) sizes as base pairs (bp) are shown on the left; NTC, no template (negative) control. **B**) Sequencing confirmed the identity of the RT-PCR product as mouse YB-1. A sequence alignment of the forward (query1, green) and reverse (query2, yellow) sequence of the PCR product with the mouse YB-1 mRNA sequence is shown; overlap between the two sequencing results is shown in blue; primer sequences are underlined; the numbers indicate the position of the sequence in the sequencing results and the mouse *YB-1* sequence (Genebank ID: BC061634.1).

Materials and Methods

Animals

All experiments were performed in accordance with the Association for Research in Vision and Ophthalmology (ARVO) statement, and the local animal ethics committee. For the investigation of YB-1 during eye development, we used C57BL/6-N mice which were inbreeds of the animal facility of the Martin-Luther University Halle (Germany). The mice were kept in a 12 h light and dark cycle with free access to food and drinking water.[21-23] After overnight mating, the day of vaginal plug formation was identified, with noon designated as embryonic day 0.5 (E0.5). The day of birth was considered postnatal day 0 (P0).

Tissue preparation

Mouse eyes of both sexes aged E13, E15, E18, P0, P7 and P14 were used as described in our earlier studies.[21,22] Briefly, for immunohistochemical analysis we washed the eyes with 4% formaldehyde fixation buffer (A+E Fischer, Wiesbaden Germany) and stored in this fixative until further use. For Western blot and RT-PCR, we isolated the retina and cornea of 20 week-old mice. For retina isolation, we induced a retinal detachment and peeled away the neuroretina from the retinal pigment epithelium (RPE). For RNA and protein extraction, retinae and corneae were stored at -80°C in lysis buffer (Macherey and Nagel Nucleospin RNA/Protein kit, Düren, Germany) until further use.

RT-PCR and cDNA sequencing

Briefly, tissue was homogenized in lysis buffer (Macherey and Nagel Nucleospin RNA/Protein kit), and RNA and protein was prepared according to the manufacturer's recommendations. RNA was quantified by UV spectroscopy, and cDNA was synthesized from 500 ng using anchored oligo-dT-primer and Script reverse transcriptase, following the manufacturer's (Jena Bioscience, Jena, Germany) manual. PCR was performed using YourTaq Direct-Load PCR Mix (biotechrabbit, Berlin, Germany) in 30 cycles (96°C for 20 s; 60°C for 20 s; 72°C for 1 min, with a final 10 min extension at 72°C) using the following primers (Eurofins MWG Operon, Ebersberg, Germany): fw1: GGAGAAGTGATG-GAGGGTGC; rev1: GGTTTAGGGTTCTCTGGGCG; fw2: AGAACGAGGGATCGGAAAGC; rev2: TGCCATCCTCTC-TAGGCTGT. The expected PCR product sizes were 248 bp, 270 bp, 136 bp, and 382 bp. All expected products span an intron and one primer (fw1) an exon/intron boundary. PCR products were separated by agarose (1.5% in TAE) gel electrophoresis and visualized using GelRed® Prestain Plus 6X DNA loading dye (VWR, Dresden, Germany) in a VWR® CHEMI Premium Imager (VWR). PCR products from the primer combination rev1/fw3 were purified by the PCR-clean up purification kit (Geneon, Ludwigshafen, Germany) and sequenced by Eurofins using the PCR primers.

Western blot analysis

The immunoblotting experiments were carried out as described in our previous studies.[22] Briefly, proteins (20 µg) were separated on a 13% denaturing polyacrylamide gel and transferred to a nitrocellulose blotting membrane (0.45 µM, Whatman) using a Bio-Rad SD blotting system, as previously described.[24] Gels contained trichloroethanol (0.5%, Sigma-Aldrich, Taufkirchen, Germany) to visualize the protein after UV irradiation for 1 mi in the imaging system.[25] Membranes were stained with Ponceau S to confirm effective transfer. Blots were blocked with BSA (2%) in TBS containing 0.2% NP-40 for 1 h at room temperature. Primary antibody was applied overnight at 4°C in the same buffer (dilution: 1:10,000). Detection was performed as previously described[24] in the imaging system.

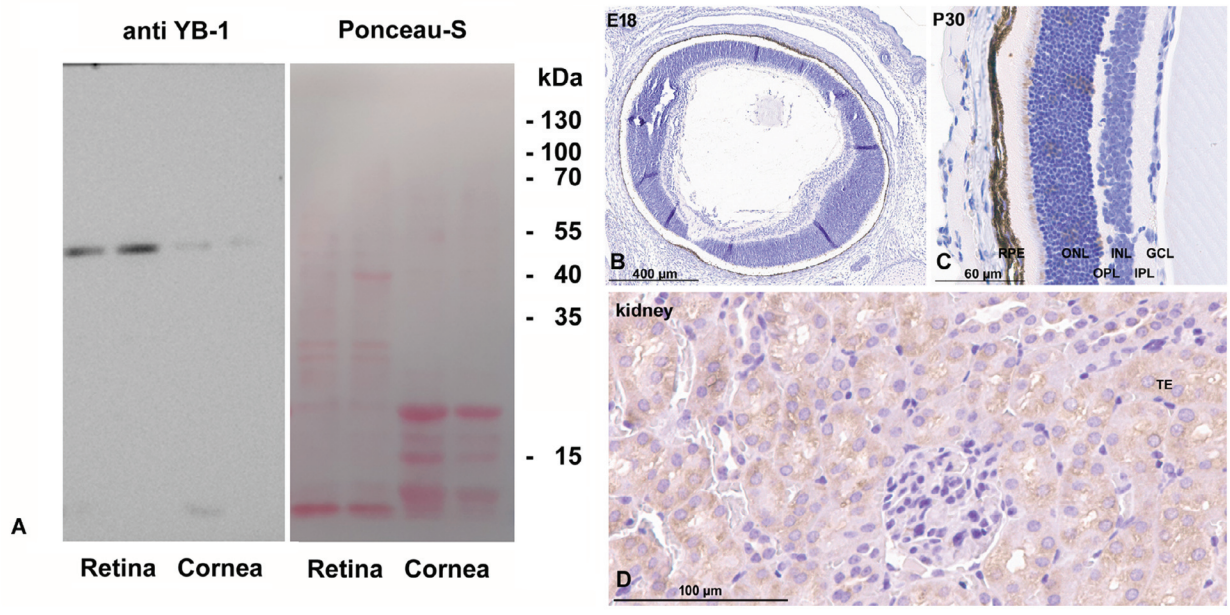

Figure 2. Western blot and controls for antibody validation. **A**) Two independent protein extracts from adult mouse retina and cornea were subjected to Western blot analysis; the result of the α-YB-1 immune-staining is shown on the left, a Ponceau-S stain of the membrane as well as Protein marker masses (kDa) on the right; a 50 kDa protein, YB-1, is present in retina and cornea. **B,C**) Negative controls were performed by omitting the primary antibody on ocular tissues from stage E18 and P30. **D**) A positive control staining was done on adult mouse kidney tissues, showing the expected weak staining of the tubular epithelium (TE).

Immunohistochemical analysis

The immunohistochemical experiments were performed as descried before.[21,22] After removing the formaldehyde (4% in PBS) under running tap water, the samples were dehydrated in graded isopropanol/water for one hour each (30%, 50%, 60%, 70% and 2x 100% isopropanol). Then, the samples were cleared in preheated paraffin/isopropanol (1:1) overnight at 65°C and were finally infiltrated with three changes of paraffin for 90-min intervals at 65°C, followed by embedding in paraffin. Sections were cut to 2-4 µm and mounted on frosted glass slides. After deparaffinization by xylene (2 times 10 min), sections were rehydrated in a graded series of ethanol (5 min each: Abs., 96%, 70%, 50%, H_2O). Heat-induced epitope recovery was carried out in citrate buffer (pH 6, 1.8 mM citric acid, 8.2 mM sodium citrate). Endogenous peroxidase activity was blocked in 3% hydrogen peroxide in PBS for 20 min. Then, unspecific antibody binding was blocked for 30 min in TBST (pH 7.4, 10 mM Tris, 136 mM NaCl, 0.05% Tween 20) supplemented with 5% non-immune serum (Vectastain ABC elite kit; Vector laboratories). Primary rabbit monoclonal antibody (Abcam 76149) diluted 1:400 in antibody dilution reagent (Ventana, Mannheim, Germany), was given to the slides at 4°C overnight. After three washes at RT in TBS containing Tween 20 (0.05%, TBST) staining was performed using a secondary, HRP conjugated antibody (Dianova, Hamburg, Germany) diluted in TBST (1/100), and a DAB detection system (Vector Laboratories, *via* Biozol, Eching, Germany). Nuclei were counterstained using Mayer's hemalaun solution (Roth, Germany). Then, slides were mounted and scanned using a Hamamatsu Nanozoomer scanner (Hamamatsu-Photonics, Japan) using a 20x lens. Negative controls were performed by omit-

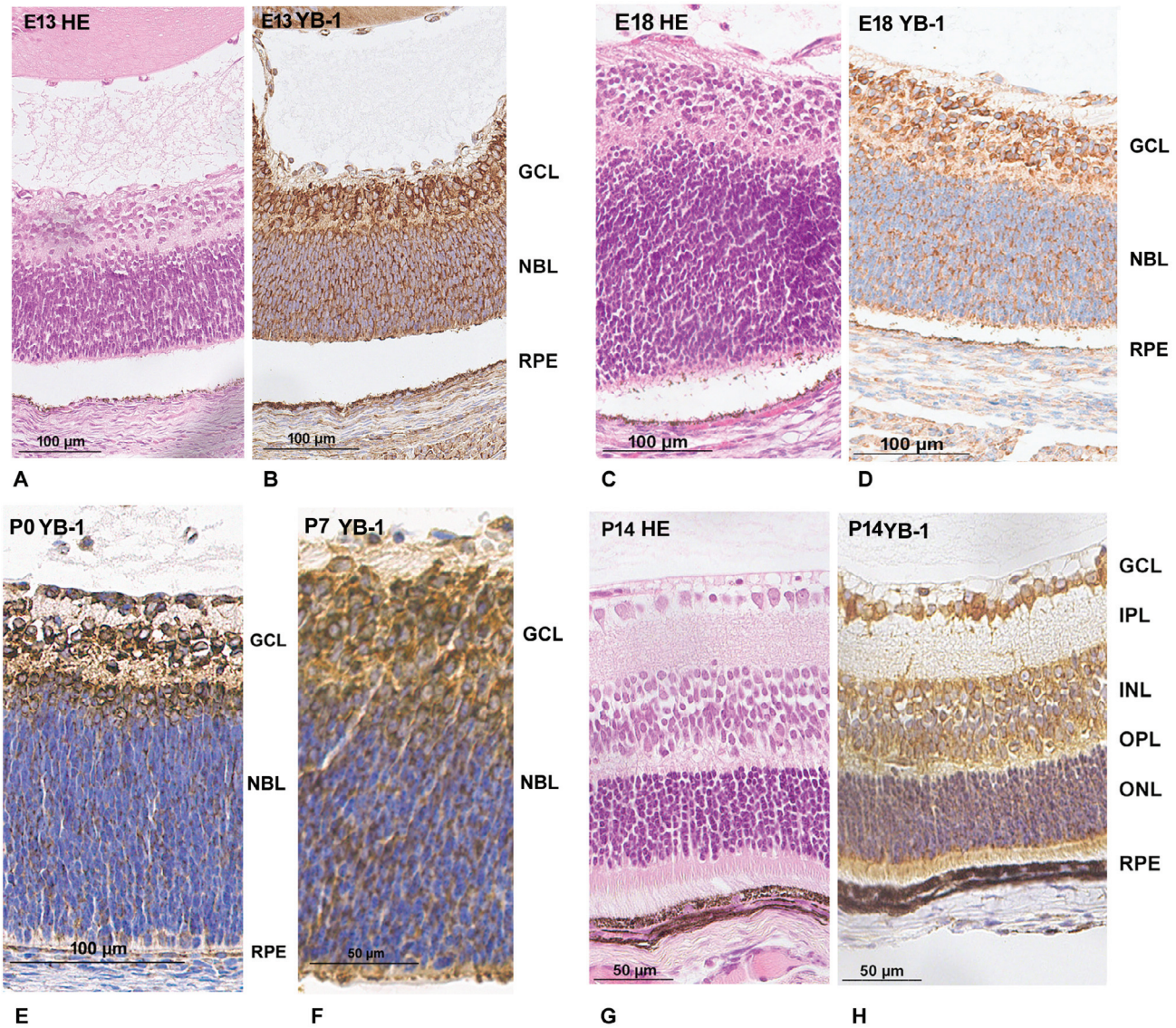

Figure 3. YB-1 protein expression in the embryonic and postnatal neuroretina detected by immunohistochemistry. Hematoxylin & Eosin staining (HE) and immunostaining YB-1 is shown. Detection of the YB-1 protein in both the neuroblastic layer (NBL) and the ganglion cell layer (GCL) of the embryonic retina (**A,B**, E12; **C,D**, E18), and post-natal stages (**E**, P0; **F**, P7) is shown. At P14 (**G,H**) expression of YB-1 is retained in all cells of the differentiated inner nuclear layer (INL) and outer nuclear layer (ONL) where photoreceptors are located. IPL, inner plexiform layer; OPL, outer plexiform layer; RPE, retinal pigment epithelium.

ting the primary antibody. Mouse kidneys (age 68 weeks) were stained using the same conditions as positive controls. QuPath (ver. 0.4.3)[26] was used to obtain semiquantitative data for the DAB staining intensity. Positive cell detection was done with a requested pixel size of 0.5 µm and a threshold of 0.05 for hematoxylin with a maximum background intensity of 2. Average DAB value per cell was then determined for two selected areas per eye, such as retina, lens epithelium, cornea and positive and negative kidney tissue. Negative controls using no primary antibody resulted in average DAB signal values of 0.063. This value was subtracted form the signal obtained with primary antibody. Tissues reaching signal values higher than the 95% confidence interval of the negative controls after subtraction of the averaged background signal (>0.02) were considered as immunopositive.

Results

Ybx1 mRNA is transcribed in the mouse retina

To evaluate the expression of Yb-1 mRNA in the mouse retina, total RNA was isolated from retinae of adult mice (20 weeks) and transcribed into cDNA using reverse transcriptase. To detect Yb-1 mRNA, the cDNA was amplified by PCR using 4 specific primers for the murine Yb-1 sequence. The amplified cDNA was separated electrophoretically in an agarose gel and stained with GelRed (Figure 1). To validate the RT-PCR results further, the largest amplification product was excised from the gel and purified for DNA sequencing. The obtained nucleotide sequence was verified using the Internet-based

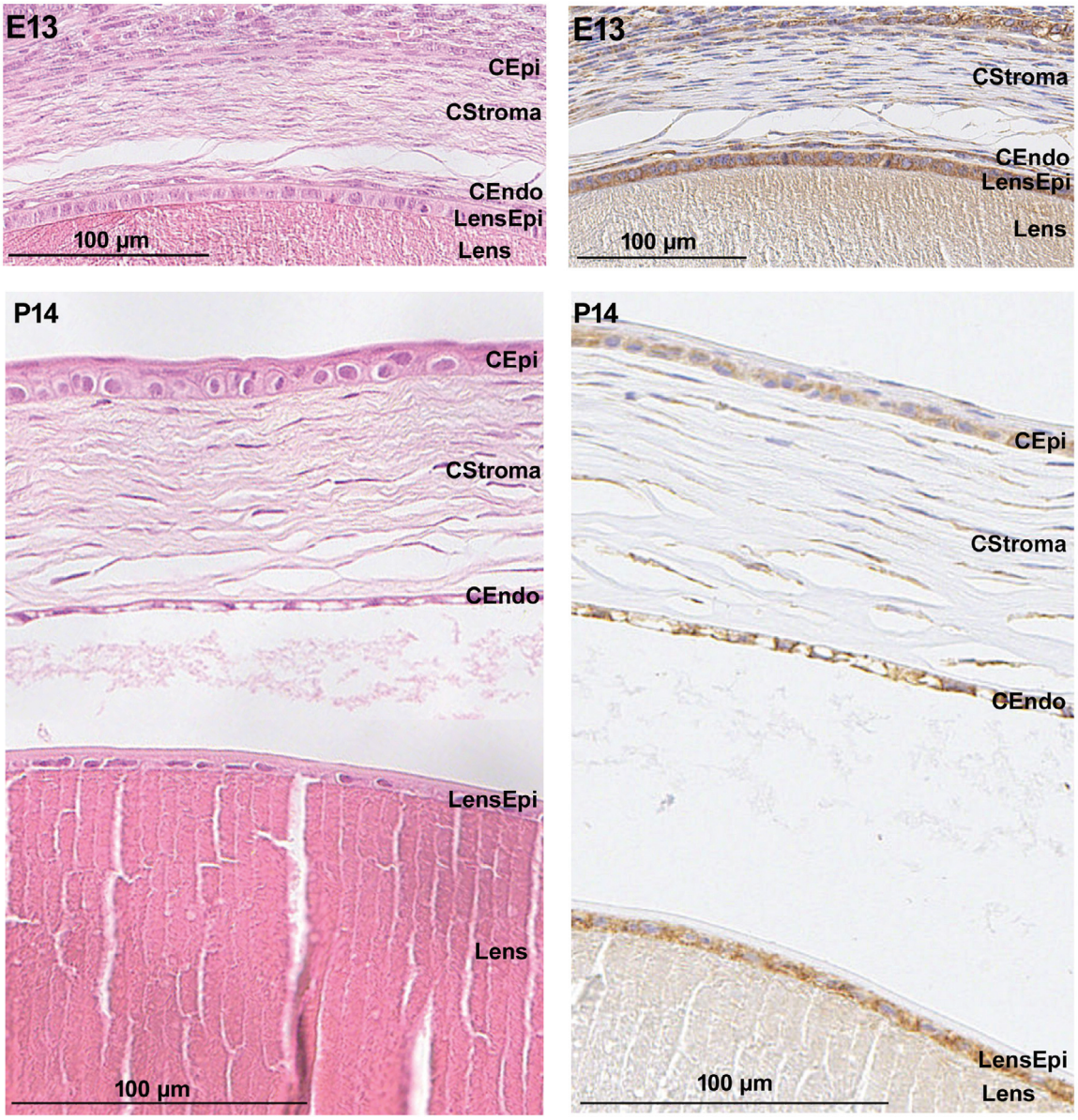

Figure 4. YB-1 protein expression in the lens and cornea detected by immunohistochemistry. Hematoxylin & Eosin staining is always shown to the left and the α-YB-1 immunostaining of the same developmental stage on the right. At E12 (upper panel), the expression of YB-1 is abundantly detectable in corneal presumptive corneal epithelial, stromal and endothelial cells as well as in lens epithelium. This expression pattern of YB-1 is maintained in the developing corneal and lens cells (lower panel) of P14. CEpi, corneal epithelium; CStroma, corneal stroma; CEndo, corneal endothelium; LensEpi, lens epithelium.

software BLAST (Basic Local Alignment Search Tool) of the National Center for Biotechnology Information (NCBI).[27] The sequence of the cDNA in the gel was found to correspondent to the published sequence of Yb-1 cDNA (Figure 1). Collectively, the data from the RT-PCR and subsequent sequence analysis demonstrated that Yb-1 mRNA is transcribed in the mouse retina.

Yb-1 protein is expressed in the neuroretina

To detect YB-1 protein in the mouse retina, we performed immunoblotting on protein extracts from mouse neuroretina and cornea. Using the anti-YB-1 antibody, we detected a single signal at about 50 kDa in protein extracts from the retina and also the cornea (Figure 2). Although the calculated mass is about 36 kDa, this size was observed in other studies before[28] and attributed to posttranslational modifications. Thus, the YB-1 protein is expressed in the mouse retinal neuroepithelium and also the cornea. Notably, the Westen blot signal for corneal protein was much lower than observed in retinal tissue.

Yb-1 is expressed during mouse retinal development

We next performed immunohistochemistry to examine the temporal and spatial expression of Yb-1 in the retinal neuroepithelium during retinal development. Adult mouse kidney samples served as a positive control tissue for Yb-1 expression (Figure 3). Yb-1 expression could be detected already from E13 in all cells of the differentiating GCL and of the neuroblastic layer (NBL) (Figure 4). In addition, Yb-1 expression was detected in all cells of the GCL, INL and ONP throughout all stages of retinal development (Figure 4) and in juvenile (P14) tissues. Thus, Yb-1 is expressed in both differentiated retinal cells and their progenitors during mouse retinal development and this is retained in juvenile eye tissues (P14). Quantification of the slides showed no significant differences in the staining intensity at the developmental stages of the retinae analyzed (Figure 5).

YB-1 is expressed during mouse corneal and lens development

To evaluate the expression of YB-1 in cornea and lens during development and in adulthood we extended the immunohistochemial analysis on these tissues from E13 to P14. Figure 4 shows that antibody staining against YB-1 detects its expression already from E13 in the presumptive CEpi, CS and CEndo as well as in lens epithelium (Figure 4). This expression is maintained in the CEpi, keratocytes, CEndo cells and lens epithelium of postnatal stages (Figure 4). Quantification of the DAB signal (Figure 5) demonstrated significantly weaker staining of corneal cells than of the lens epithelium (Figure 5). This corresponds to the results of the Western blot (Figure 2). No significant differences were seen for the developmental stages.

Discussion

YB-1 plays a crucial role in developmental processes such as proliferation and differentiation. At the molecular level, YB-1 is involved in RNA translation and stability. Under stress conditions, YB-1 protein is particularly found in stress granules,[29,30] which serve as storage compartments for RNA.[31,32] YB-1 also interacts with proteins involved in protein biosynthesis, such as eukaryotic initiation factors.[33,34] Regarding developmental processes, YB-1 regulates neuronal cell renewal and differentiation, for instance, through interaction with the polycomb repressive complex 2 in the developing mouse brain.[35] Consequently, we hypothesized its expression in the developing eye, likely exhibiting a distinct spatial and temporal pattern, especially in cells of the developing neuroretina. However, we observed that the YB-1 protein is expressed throughout eye development, starting at E13, and its expression is maintained in P14 eyes in the cytoplasm of nearly all ocular cells

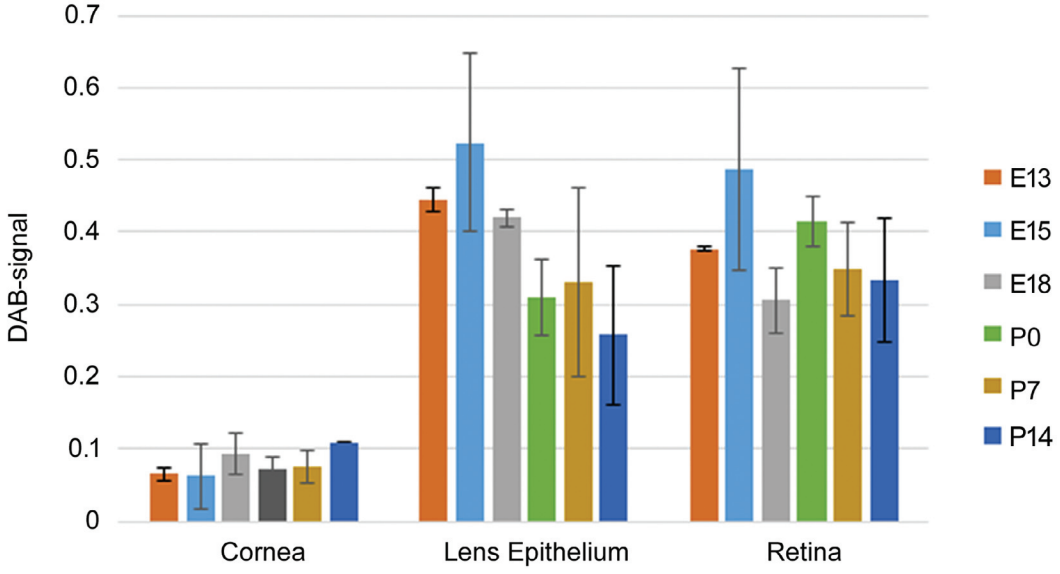

Figure 5. Quantification of DAB-staining intensity. DAB signal intensity of the immunohistochemistry (IHC) of cornea, lens epithelium and retinal tissue was quantified. Eyes of 2-3 animals per developmental stage were subjected to IHC and for two randomly selected areas each, the average cellular DAB signal was determined using the QuPath software. Average and standard deviation is shown. Signal in corneal tissue was statistically different from lens and cornea. However, there was no statistical difference between the developmental stages of lens and retina (one-way ANOVA, Games-Howell *post-hoc* test).

examined. Our protein expression data align with in-situ hybridization data,[36] although these RNA data suggested a decreased expression from P0 to P7, which reappeared in adult eyes. Because protein- and mRNA stability can significantly differ from each other, we propose that the YB-1 protein remains stable in P0 to P7 although the mRNA seems being degraded. As we did not prepare protein and RNA from these stages, we are not able to further analyze this apparent difference between protein and mRNA abundance. Nevertheless, our data show that the expression of the YB-1 protein was not limited to neuronal, differentiating, or proliferating cells.

A significant limitation of our study is that we only investigated the presence of the protein regardless posttranslational modifications. Further studies on the activation state, mediated by phosphorylation or acetylation, may provide additional insights into the function of this protein in the developing eye. A histological analysis of the retinal architecture of YB-1 knock-out mice[37] could provide further understanding of the role of YB-1 in the development of the murine eye.

In conclusion, the ubiquitous expression of the YB-1 protein in the developing mouse eye supports the notion that this protein might be essential for eye development and stress responses. Further studies are needed to clarify the role of YB-1 during eye development.

Acknowledgements

The authors thank the Immunohistochemistry Laboratory of the Institute of Pathology, Magdeburg and Brandenburg/Havel for preparing the slides for staining.

References

1. Graw J. Eye development. Curr Top Dev Biol 2010;90:343-86.
2. Hoon M, Okawa H, Della Santina L, Wong RO. Functional architecture of the retina: development and disease. Prog Retin Eye Res 2014;42:44-84.
3. Chang W, Zhao Y, Rayee D, Xie Q, Suzuki M, Zheng D, et al. Dynamic changes in whole genome DNA methylation, chromatin and gene expression during mouse lens differentiation. Epigenetics Chromatin 2023;16:4.
4. Balazs EA, Toth LZ, Ozanics V. Cytological studies on the developing vitreous as related to the hyaloid vessel system. Albrecht Von Graefes Arch Klin Exp Ophthalmol 1980; 213:71-85.
5. Ito M, Nakashima M, Tsuchida N, Imaki J, Yoshioka M. Histogenesis of the intravitreal membrane and secondary vitreous in the mouse. Invest Ophthalmol Vis Sci 2007;48:1923-30.
6. Miesfeld JB, Brown NL. Eye organogenesis: A hierarchical view of ocular development. Curr Top Dev Biol 2019;132:351-93.
7. Byerly MS, Blackshaw S. Vertebrate retina and hypothalamus development. Wiley Interdiscip Rev Syst Biol Med 2009;1: 380-9.
8. Cayouette M, Poggi L, Harris WA. Lineage in the vertebrate retina. Trends Neurosci 2006;29:563-70.
9. Cepko C. Intrinsically different retinal progenitor cells produce specific types of progeny. Nat Rev Neurosci 2014;15: 615-27.
10. Marquardt T, Gruss P. Generating neuronal diversity in the retina: one for nearly all. Trends Neurosci 2002;25:32-8.
11. Swamynathan SK. Ocular surface development and gene expression. J Ophthalmol 2013;2013:103947.
12. Pajoohesh-Ganji A, Stepp MA. In search of markers for the stem cells of the corneal epithelium. Biol Cell 2005;97:265-76.
13. Zhu CC, Dyer MA, Uchikawa M, Kondoh H, Lagutin OV, Oliver G. Six3-mediated auto repression and eye development requires its interaction with members of the Groucho-related family of co-repressors. Development 2002;129:2835-49.
14. Bohm EW, Buonfiglio F, Voigt AM, Bachmann P, Safi T, Pfeiffer N, et al. Oxidative stress in the eye and its role in the pathophysiology of ocular diseases. Redox Biol 2023;68: 102967.
15. Ankamah E, Sebag J, Ng E, Nolan JM. Vitreous antioxidants, degeneration, and vitreo-retinopathy: exploring the links. Antioxidants (Basel) 2019;9:7.
16. Lyabin DN, Eliseeva IA, Ovchinnikov LP. YB-1 protein: functions and regulation. Wiley Interdiscip Rev RNA 2014;5:95-110.
17. Lindquist JA, Mertens PR. Cold shock proteins: from cellular mechanisms to pathophysiology and disease. Cell Commun Signal 2018;16:63.
18. Shah A, Lindquist JA, Rosendahl L, Schmitz I, Mertens PR. Novel insights into YB-1 signaling and cell death decisions. Cancers (Basel) 2021;13:3306.
19. Xue X, Huang J, Yu K, Chen X, He Y, Qi D, et al. YB-1 transferred by gastric cancer exosomes promotes angiogenesis via enhancing the expression of angiogenic factors in vascular endothelial cells. BMC Cancer 2020;20:996.
20. Shaughnessy M, Wistow G. Absence of MHC gene expression in lens and cloning of dbpB/YB-1, a DNA-binding protein expressed in mouse lens. Curr Eye Res 1992;11:175-81.
21. Sel S, Kalinski T, Enssen I, Kaiser M, Nass N, Trau S, et al. Expression analysis of ADAM17 during mouse eye development. Ann Anat 2012;194:334-8.
22. Sel S, Munzenberg C, Nass N, Kalinski T, Datan M, Auffarth GU, et al. The transcription factor Foxk1 is expressed in developing and adult mouse neuroretina. Gene Expr Patterns 2013;13:280-6.
23. Sel S, Patzel E, Poggi L, Kaiser D, Kalinski T, Schicht M, et al. Temporal and spatial expression pattern of Nnat during mouse eye development. Gene Expr Patterns 2017;23-24:7-12.
24. Behringer A, Stoimenovski D, Porsch M, Hoffmann K, Behre G, Grosse I, et al. Relationship of micro-RNA, mRNA and eIF expression in tamoxifen-adapted MCF-7 breast cancer cells: impact of miR-1972 on gene expression, proliferation and migration. Biomolecules 2022;12:916.
25. Ladner-Keay CL, Turner RJ, Edwards RA. Fluorescent protein visualization immediately after gel electrophoresis using an in-gel trichloroethanol photoreaction with tryptophan. Methods Mol Biol 2018;1853:179-90.
26. Bankhead P, Loughrey MB, Fernandez JA, Dombrowski Y, McArt DG, Dunne PD, et al. QuPath: Open source software for digital pathology image analysis. Sci Rep 2017;7:16878.
27. Altschul SF, Gish W, Miller W, Myers EW, Lipman DJ. Basic local alignment search tool. J Mol Biol 1990;215:403-10.
28. Zhao S, Wang Y, Guo T, Yu W, Li J, Tang Z, et al. YBX1 regulates tumor growth via CDC25a pathway in human lung adenocarcinoma. Oncotarget 2016;7:82139-57.
29. Guarino AM, Mauro GD, Ruggiero G, Geyer N, Delicato A, Foulkes NS, et al. YB-1 recruitment to stress granules in zebrafish cells reveals a differential adaptive response to stress. Sci Rep 2019;9:9059.
30. Lyons SM, Achorn C, Kedersha NL, Anderson PJ, Ivanov P. YB-1 regulates tiRNA-induced Stress Granule formation but not translational repression. Nucleic Acids Res 2016;44:6949-60.
31. Somasekharan SP, El-Naggar A, Leprivier G, Cheng H, Hajee

S, Grunewald TG, et al. YB-1 regulates stress granule formation and tumor progression by translationally activating G3BP1. J Cell Biol 2015;208:913-29.
32. Tanaka T, Ohashi S, Kobayashi S. Roles of YB-1 under arsenite-induced stress: translational activation of HSP70 mRNA and control of the number of stress granules. Biochim Biophys Acta 2014;1840:985-92.
33. Ivanova IG, Park CV, Yemm AI, Kenneth NS. PERK/eIF2alpha signaling inhibits HIF-induced gene expression during the unfolded protein response via YB1-dependent regulation of HIF1alpha translation. Nucleic Acids Res 2018;46:3878-90.
34. Vo DK, Engler A, Stoimenovski D, Hartig R, Kaehne T, Kalinski T, et al. Interactome mapping of eIF3A in a colon cancer and an immortalized embryonic cell line using proximity-dependent biotin identification. Cancers (Basel) 2021;13:1293.
35. Evans MK, Matsui Y, Xu B, Willis C, Loome J, Milburn L, et al. Ybx1 fine-tunes PRC2 activities to control embryonic brain development. Nat Commun 2020;11:4060.
36. Blackshaw S, Harpavat S, Trimarchi J, Cai L, Huang H, Kuo WP, et al. Genomic analysis of mouse retinal development. PLoS Biol 2004;2:E247.
37. Bernhardt A, Haberer S, Xu J, Damerau H, Steffen J, Reichardt C, et al. High salt diet-induced proximal tubular phenotypic changes and sodium-glucose cotransporter-2 expression are coordinated by cold shock Y-box binding protein-1. FASEB J 2021;35:e21912.

Received: 4 June 2025. Accepted: 29 September 2025.

European Journal of Histochemistry 2025; 69:4244
doi:10.4081/ejh.2025.4244